أكاديمية كاوست
KAUST ACADEMY

جامعة الملك عبدالله للعلوم والتقنية
King Abdullah University of Science and Technology

Final Project Report

Summer School – Final Report

Cosolvency-Driven Growth of $MAPbI_3$ Single-Crystal Solar Cells using inverse temperature crystallization method (ITC)

Student: Munira Alruwaili

A report submitted in partial fulfilment of the requirements of the **Summer School, Energy Transition Specialization (WE Spark)**

Supervisor: Mudeha Khan

Center for Renewable Energy and Storage Technologies (CREST),
Division of Physical Sciences and Engineering
King Abdullah University of Science and Technology (KAUST), Thuwal

August 26, 2025

I. Introduction and Project Objectives

$MAPbI_3$ single-crystal perovskite solar cells ($MAPbI_3$-SCPSCs) exhibit low defect density, long carrier diffusion lengths, high carrier mobility, and extended lifetimes. These characteristics reduce charge recombination and improve efficiency compared to polycrystalline films, making single crystals a promising platform for next-generation perovskite photovoltaics.

The main objectives of this project are:

1. To enhance precursor solubility for controlled crystal growth.
2. To precisely control the crystallization process to obtain high-quality $MAPbI_3$ single crystals.
3. To fabricate single crystals using the inverse temperature crystallization (ITC) method.
4. To characterize the crystals and devices through scanning electron microscopy (SEM), and current–voltage (I–V) measurements.

II. Current Progress and Milestones

$MAPbI_3$ single crystals were successfully grown using a cosolvency-assisted ITC method. While γ-butyrolactone (GBL) alone produced moderate-quality crystals, the addition of 2-methoxyethanol (2-ME) enhanced precursor solubility. This combination resulted in larger, more uniform single crystals with fewer defects.

Solar cells fabricated from these cosolvent-grown crystals exhibited improved performance compared to those grown in GBL only. Specifically, Jsc increased from 20.82 to 22.36 mA/cm^2, Voc from 1.01 to 1.10 V, and FF from 66.75% to 75.48%, leading to an increase in PCE from 14.12% to 18.58%. These results highlight the effectiveness of cosolvency in controlling crystallization and improving device performance.

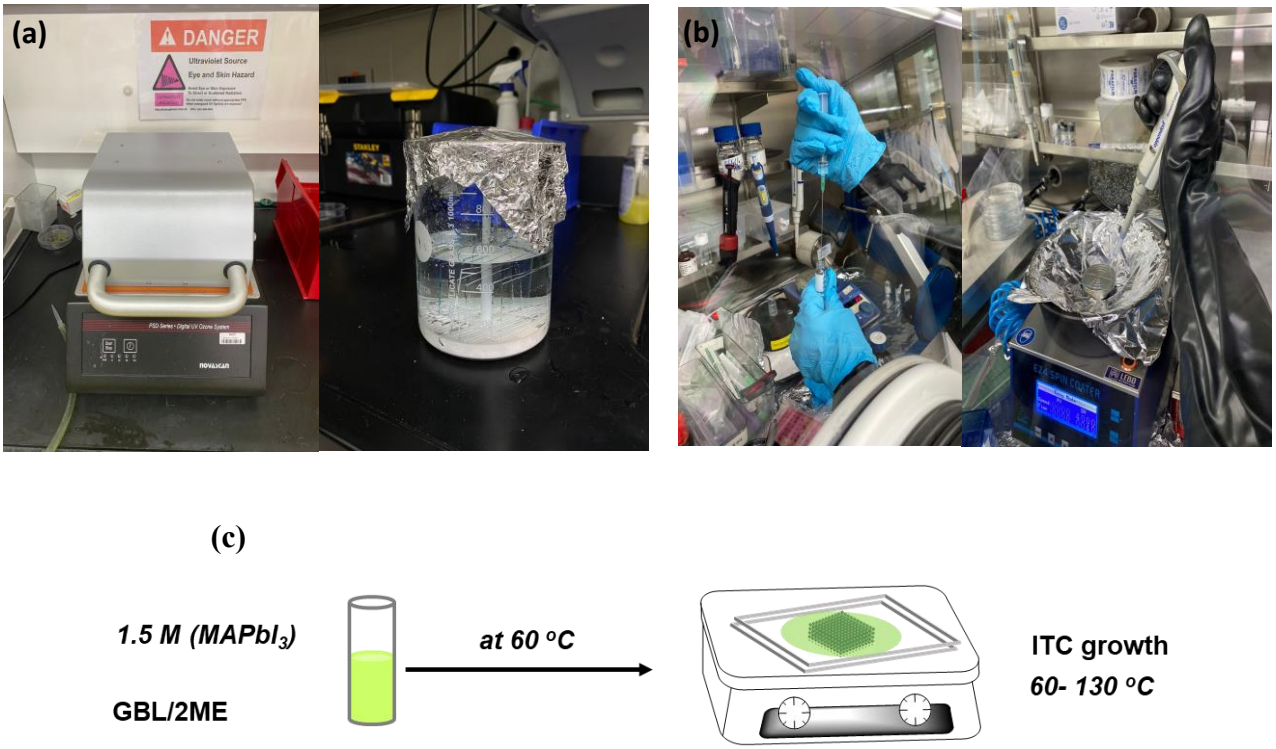


Figure 1 shows the fabrication of single-crystal $MAPbI_3$ perovskite solar cells. Substrates were cleaned by sequential sonication and UV treatment (Figure 1a), followed by spin coating of PTAA as the hole transport layer on ITO (Figure 1b). Single crystals were then grown using the inverse temperature crystallization (ITC) method in a confined space (Figure 1c).

III. Methodology and Approach

Chemical Precursors and Solvents: Methylammonium iodide (MAI) and lead iodide (PbI_2) were dissolved in a mixture of γ-butyrolactone (GBL) and 2-methoxyethanol (2-ME). GBL alone offers high solubility, which can cause excessive nucleation and small crystals, while 2-ME alone has low solubility, leading to rapid and irregular crystallization. The mixed solvent provided controlled nucleation and stable growth of large single crystals.

Single-Crystal Growth (Space-Confined ITC): The precursor solution was sandwiched between two ITO substrates coated with a hydrophobic hole transport layer (PTAA). Gradual heating from 60 °C to 130 °C induced crystallization. After cooling to 60 °C, the glasses were separated, and the crystals were allowed to reach room temperature. Fabrication, storage, and testing were performed in a nitrogen-filled glovebox to prevent moisture-related defects and poor interface formation.

Device Fabrication:

1. Substrate Cleaning: ITO-coated glass substrates were cleaned sequentially in detergent, deionized water, acetone, and isopropyl alcohol, each for 15 min in an ultrasonic bath, followed by nitrogen drying and UV–ozone treatment.
2. Hole Transport Layer: PTAA was spin-coated at 3000 rpm for 30 s and annealed at 100 °C for 10 min.

3. Perovskite Layer: $MAPbI_3$ single crystals were grown via the space-confined ITC method described above.
4. Electron Transport Layer and Electrodes: C_{60} and BCP were deposited by thermal evaporation, followed by Cu top electrodes.

Characterization: Optical microscopy and SEM were used to analyze morphology and crystal integration. I–V measurements were performed under controlled nitrogen conditions to evaluate device performance.

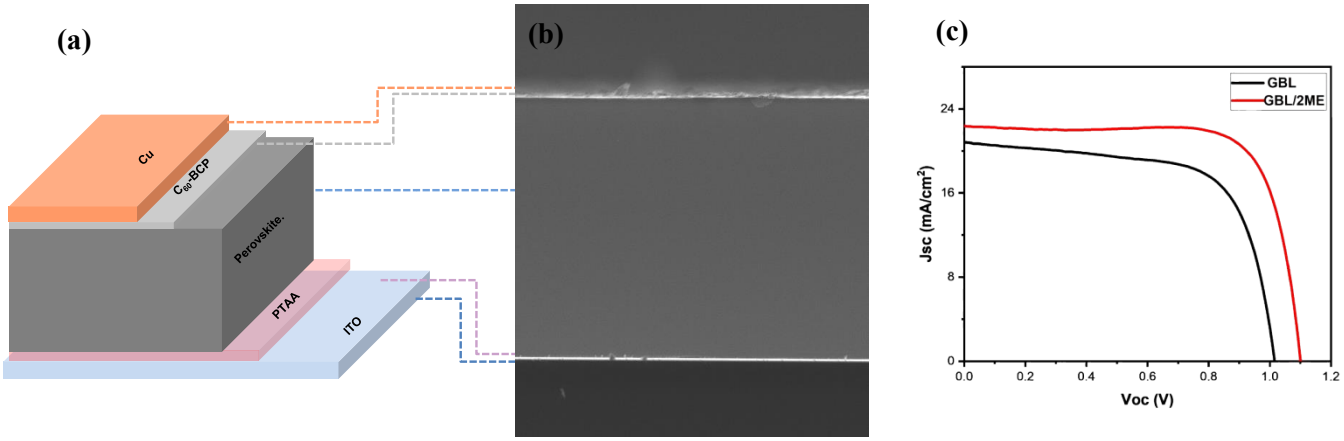


Figure 2. Device structure and photovoltaic parameters. (a) Schematics showing our device architecture. (b) SEM cross-section of device. (c) J–V characteristics.

IV. Preliminary Results and Findings

Inverted (p–i–n) single-junction devices were fabricated with architecture ITO/PTAA/$MAPbI_3$/C_{60}/BCP/Cu. The cross-section SEM image (Figure 2b) shows a uniform perovskite thickness of approximately 20 μm, indicating high-quality crystal growth and proper layer integration.

J–V characterization (Figure 2c) revealed that cosolvent-grown crystals significantly outperformed GBL-only crystals:

- Jsc: 20.82 → 22.36 mA/cm²
- Voc: 1.01 → 1.10 V
- FF: 66.75% → 75.48%
- **PCE: 14.12% → 18.58%**

These results confirm that the 2-ME cosolvent enhances crystallization control, reduces defects, and improves interfacial contact, which directly translates to higher device efficiency.

V. Challenges and Obstacles Encountered

Several challenges influenced crystal growth and device fabrication:

- Limited project timeframe required precise planning and scheduling.
- Maintaining the correct GBL/2-ME ratio was critical to avoid excessive or irregular nucleation.
- Temperature control during ITC was essential to reduce defects.
- Removing residual precursor solution without damaging crystals required repeated practice.

VI. Next Steps and Future Work

Future work will focus on advanced characterization and device optimization:

- **Characterization:** Photoluminescence (PL), UV–vis absorption, and time-resolved spectroscopy to study carrier dynamics and optoelectronic properties.
- **Device Optimization:** Refining crystal thickness and uniformity, surface/interface passivation at PTAA/$MAPbI_3$ and $MAPbI_3/C_{60}$, and improving transport layers and Cu contacts to increase Voc and FF.
- **Material Improvements:** Exploring mixed-cation (MA/FA) strategies to enhance stability and reduce degradation and investigating reduced-lead compositions for environmental safety.

VII. Resources and Tools Used

Chemical Precursors: MAI and PbI_2 dissolved in GBL/2-ME.
Substrates and Functional Layers: ITO-coated glass, PTAA (HTL), C_{60}/BCP (ETL), Cu electrodes.
Fabrication Equipment: Nitrogen glovebox, ultrasonic bath, spin coater, hotplate (ITC), thermal evaporator, UV–ozone cleaner.
Characterization Tools: Optical microscopy, SEM, and I–V measurement setup.

References

(1) Moazzezi, P.; Yeddu, V.; Cheong, I. T.; Kokaba, M. R.; Dayneko, S.; Ahmed, Y.; Saidaminov, M. I. Discovery of Perovskite Cosolvency and Undoped $FAPbI_3$ Single-Crystal Solar Cells Fabricated in Ambient Air**.** ***J. Am. Chem. Soc.*** **2025**, *147* (12), 10203−10211.

(2) Khan, M.; Maity, P.; Almasabi, K.; Hasanov, B. E.; Lintangpradipto, M. N.; Zhou, R.; Mir, W. J.; Sheikh, T.; Emwas, A.; Hedhili, M. N.; Abulikemu, M.; Mohammed, O. F.; Bakr, O. M. Surface Planarization and Chemical Adhesion Enable 25.0% Efficient Perovskite Single-Crystal Solar Cells. ***ACS Mater. Lett.*** **2025**, *7*, 1603−1611.

(3) Yuan, L.; Xue, Q.; Wang, F.; Li, N.; Waterhouse, G. I. N.; Brabec, C. J.; Gao, F.; Yan, K. Perovskite Solar Cells and Light-Emitting Diodes: Materials Chemistry, Device Physics and Relationship. ***Chem. Rev.*** **2025**, *125*, 5057−5162.

(4) Li, C.; Chen, C. Single-Crystal Perovskite for Solar Cell Applications. ***Small*** **2024**, *20*, 2402759.

(5) De Marco, L.; Nasti, G.; Abate, A.; Rizzo, A. Perovskite Single-Crystal Solar Cells: Advances and Challenges. ***Sol. RRL*** **2022**, *6*, 2101085.

(6) Chen, Z.; Turedi, B.; Alsalloum, A. Y.; Yang, C.; Zheng, X.; Gereige, I.; AlSaggaf, A.; Mohammed, O. F.; Bakr, O. M. Single-Crystal $MAPbI_3$ Perovskite Solar Cells Exceeding 21% Power Conversion Efficiency. ***ACS Energy Lett.*** **2019**, *4*, 1258−1259.